Impurity Distribution in Al_2O_3 formed on an FeCrAl Alloy

P. Y. Hou, X. F. Zhang and R. M. Cannon

Materials Sciences Division
Lawrence Berkeley National Laboratory
MS 62-203, 1 Cyclotron Rd., Berkeley, CA 94720, USA

Abstract

Analytical electron microscopy and Auger spectroscopy were used to study the amount and distribution of Fe, Cr and S impurities in the Al_2O_3 scale grown on an FeCrAl alloy. Segregations of Fe on grain boundaries and S on internal void surfaces were found, and a mechanism of intragranular void formation in Al_2O_3 is proposed.

Keywords: oxidation, iron alloys, alumina, analytical electron microscopy, AES.

1. Introduction

The growth of α-Al_2O_3 scales that form on FeCrAl alloys during high temperature oxidation is generally considered to be controlled by oxygen inward diffusion through oxide grain boundaries [1,2]. Aluminum also diffuses out, which can cause growth within the scale [3]. The degree of Al outward transport can be significantly reduced by the presence of reactive elements, such as Y, Hf or Zr [1,2], which segregate to Al_2O_3 grain boundaries [4]. However, the extent of outward growth seems to differ appreciably among several reactive-element doped Fe based alloys [5]. Similar conclusions have been drawn from creep studies, where the addition of Zr, Nd, Y, or La in bulk Al_2O_3 decreases the creep rate (roughly in the order given) and is believed to reduce the Al grain boundary diffusivity [6,7]. Other dopants, such as Fe and Ti, were found to increase creep rates instead, but it is unclear whether they affect the aluminum lattice [8,9] or boundary diffusion [10] rates. These creep results all point to a strong dependence of the Al_2O_3 transport properties on dopant types and even concentrations [8,9]. Similar effects should exist during alumina scale growth, as there is a large source of foreign atoms in the underlying alloy that can be incorporated into the scale. These effects are important as the magnitudes of the diffusivities influence the oxidation rates, and the relative magnitude of the cation and anion diffusion rates influence scale wrinkling or other substrate distortion [11].

The most abundant impurities in a growing Al_2O_3 scale must be the base metals from the alloy, which are often incorporated during the initial stage of oxidation [2]. Although this fact is well known, their distribution in the scale as it thickens has not been systematically studied. Another possible impurity in the scale is sulfur, which is typically present in tens of ppm levels in commercial alloys. This sulfur has been shown to segregate strongly to the Al_2O_3/FeCrAl interface [12], but it is uncertain whether it would either diffuse or be carried into the scale. Some have suggested that it segregates at the oxide grain boundary and thereby reduce the

scale growth rate [13,14]; yet there has been little evidence to support this proposal. Before any conclusions can be drawn on the important question of whether and how these elements may affect transport through Al_2O_3 scales, it is imperative to first determine their distribution within the scale as a function of scale growth. The purpose of this work, therefore, is to study the distribution of Fe, Cr, S and any other noticeable impurities in Al_2O_3 scales grown on an FeCrAl alloy at different temperatures and times using analytical transmission electron microcopy (TEM) and scanning Auger electron spectroscopy (AES).

2. Experimental methods

A high purity Fe-18.4Cr-9.2Al (at%) alloy, with 52 ppm sulfur and a total impurity level of 0.16%, was used for this study. The alloy was made by induction melting, followed by cutting then annealing at 1100°C. Specimens typically 15x10x1mm were polished to a 1 μm surface finish, cleaned, then placed in an alumina boat and oxidized. Most oxidation took place in flowing dry O_2 at 1000°C; a few specimens were oxidized at 1200°C in O_2 or in ambient air.

AES depth profiling through thin scales oxidized for short times at 1000°C was used to study the scale composition during early stages of oxidation. Thicker scales that spalled during sample cooling (4-6 μm thick) were collected and fractured inside the ultra high vacuum (UHV) chamber to evaluate the composition at the fractured Al_2O_3 grain boundaries by AES. Some of the pieces were also mounted on Au washers for ion-mill thinning from both sides for subsequent observations using TEM. Thin scales that formed after short time oxidation were mounted on gold washers, after they were spalled by indentation or stub pulling, and were ion milled as necessary if thin regions were not produced by the fracture. Cross sectional specimens were not used to avoid contamination from Fe and Cr in the alloy during ion thinning of specimens.

TEM analyses were carried out using a 200 kV Philips CM200 microscope, to determine the average grain size, composition and structure of the scales. Polycrystalline ring patterns from electron diffraction of 30 μm diameter areas were used to identify the Al_2O_3 structure and measure lattice parameters. Chemical microanalyses were performed by X-ray energy-dispersive spectroscopy (EDS). Spectra were collected using a windowless detector, and processed with ES Vision 4.0 software. For quantification of impurities, the K_α peaks of detected elements, Fe, Cr, S, and Al, were integrated, after absorption and fluorescence corrections, background subtraction, and Gaussian peak fitting. The dominant Al-K_α peak was used as a reference. Thus, Fe/Al, Cr/Al, and S/Al ratios, obtained using the Cliff-Lorimer equation [15], led to determination of the impurity contents. Point-EDS analyses with an electron beam typically focused to a 17 nm diameter circular probe allowed direct comparison of the impurity contents at grain boundaries from that in adjacent grains. Electron beam broadening through the 50-100 nm foil thickness was accounted using the single scattering model. Large area analysis, i.e., 14 μm diameter, was used to obtain an average concentration of impurities in the scale.

3. Results and Discussion

3.1 Base metal incorporation and its effect on transport

Scale composition during the initial stage of oxidation was studied using AES depth profiling (Fig. 1). Before heat treatment, an oxide a few nm thick existed on the sample surface. This oxide contained Fe, Cr and Al where Fe is enriched at the outer portion and Cr at the inner portion. Exposure to high temperatures caused immediate thickening of the Fe and Cr oxide while Al started to enrich in the oxide near the scale/alloy interface. Further oxidation resulted in a complete Al_2O_3 surface layer, and, moreover, the initially formed Fe and Cr oxides became fully incorporated into it. Studies reported elsewhere for FeCrAl alloys revealed that after some minutes at 1000°C, the transient oxides that initially formed had largely been converted to the α-Al_2O_3 structure [16], i.e., by the time for the spectra in Fig. 1(c). Integrating the depth profile curves with distance, the relative change of scale composition with oxidation time (or scale thickness) can be determined and the results are shown in Fig. 1(d). The first-formed scale is clearly seen to contain a large amount of Fe and Cr, which quickly became incorporated into and then diluted in a continuously growing α-Al_2O_3 scale.

The most abundant impurities in the Al_2O_3 scales as detected by TEM were also Fe and Cr. Sulfur was found only occasionally, which will be discussed later. No other impurities were detected. The detectability of an element in Al_2O_3 is ~0.1 at% and increases with increasing atomic weight. Under the 17 nm beam used experimentally and assuming a scale thickness of 100 nm, if all the impurity were at the grain boundary, these limits would correspond to impurity adsorption levels ranging from 0.51 atoms/nm^2 for Fe to 0.54 nm^{-2} for Ca [17]. Using an interface density of 10 atoms/nm^2, these numbers correspond to ~0.05 monolayer at the grain boundary.

The EDS results of the average Fe and Cr concentrations in the scale as a function of scale thickness from different TEM specimens are summarized in Table 1. The scales examined by TEM, all identified as α-Al_2O_3, were thicker than those studied using AES depth profile, but consistently the average amounts of Cr and Fe in them continually decreased with scale thickness. The oxide grain size almost doubled over 0.5 to 26 hrs at 1000°C, and more grain growth was observed at 1200°C. The α-Al_2O_3 unit cell was enlarged, particularly along its c-axis. The degree of enlargement was proportional to the amount of Fe and Cr present, indicating that some of these elements were dissolved in the alumina lattice. Low magnification analyses always gave uniform Fe and Cr distributions, but point analysis at different regions often showed large variations, which was not due to the presence of any second phase particles. This may be related to a non-uniform distribution of the initially formed Fe and/or Cr-containing oxide.

Under these conditions, segregation of Fe or Cr at the grain boundaries was studied by comparing point analyses made at a boundary and within the grains adjacent to it. An average of 38% of the boundaries had higher concentrations of Fe compared to the adjacent grain interiors, but none exhibited Cr enrichment. The maximum Fe enrichment was found to be 1.4

at% in excess of the amount in the grains, ~ 7 atom/nm^{-2}. As the scales thicken and average Fe levels decrease, the segregation levels should decline; however, quantification of the difference between grain and boundary is imprecise because the grains contain some Fe and detection levels for Fe segregation exceed the level mentioned previously (0.5 nm^{-2}). Indeed the thickest scale (1200°C/120h) was nearly free from any detectable impurities. The grain faces of these thickest scales exposed in UHV on fracture cross-sections also did not contain any detectable impurities, over the entire scale cross-section. The detectability of Fe on Al_2O_3 by AES is about 0.24 monolayer and the level is 0.03 for S.

Since Cr_2O_3 forms a complete solid solution with Al_2O_3 at elevated temperatures [18], it is expected to dissolve and not segregate strongly at grain boundaries. Fe, on the other hand, evidently segregated to some grain boundaries. In the Al_2O_3 scale, Fe can exist as Fe^{2+} or Fe^{3+}. The latter has an appreciable solubility in Al_2O_3, about 3-5 at% at the temperatures of interest [19], but the former is only soluble at ppm levels [20]. This solubility difference suggests that Fe^{2+} is the ion that should segregate. Under the oxygen potential gradient across the alumina scale, Fe^{2+} is expected to exist closer to the scale/alloy interface (where the oxygen activity is very low). Future work should involve EELS to differentiate the charge states of the Fe and study the segregation distribution across the thickness of the scale.

Results from both AES and TEM studies have shown that Al_2O_3 scales became purer as they thickened with oxidation time. The oxide grain size, at 1000°C, did not change noticeably from 1-26 hours (Table 1), but the parabolic oxidation rate parameter-decreased by a factor of two during this time [21]. Similar results showing a decreasing Al_2O_3 growth rate parameter with time have also been reported by others [14]. This decrease may very well be associated with an effect of impurities on grain boundary transport, particularly that of Fe, since its concentration in the scale decreases with time during this period and it is the only element found to segregate with appreciable amounts at grain boundaries. A faster Al transport due to the presence of Fe in the scale is in agreement with the fact that Fe additions increase Al_2O_3 creep rates [8-10]. Such an enhancement would also explain the extensive lateral growth found on FeCrAl alloys during the early stage of oxidation that causes scale convolutions [22,11]. The lateral growth is a result of O and Al reacting within the oxide [3], the extent of which should increase with higher transport rates of Al. However, in a note of caution, it is recognized that the evidence for faster creep rates with Fe present is only unambiguous in a regime controlled by lattice diffusion rather than boundary diffusion [8-10].

3.2 S in the scales and the mechanism of intragranular pore formation

Sulfur was not detected by TEM in any of the scales that spalled either during cooling or induced by indentation, except at pore surfaces and at one grain boundary where it was also enriched with Cr. No other boundaries exhibited detectable S, although many grains and grain boundaries on scales from several samples were carefully analyzed. However, when an entire piece of scale was pulled away from the substrate using an adhesive, S was found everywhere on the metal side and occasionally on the oxide side of the interface. Possibly, depending on the fracture method, some of the sulfur that segregated at the interface can remain on the oxide side

when the scale spalls. This may be related to the fracture path at the interface along the 2-3 atom layers of segregated sulfur [12]. Similar behavior has been noted before from AES examinations of the scale underside in UHV [12].

While examining thin sections of Al_2O_3 scales, sub-micron sized voids were often found, and most of them were located within the grains (Fig. 2). This morphology has been shown before [23,24], but chemical analysis around the pores has never been made. Using the small probe EDS analysis, compositions around many of these voids were determined. It was found that all of them at some location on their surfaces contained noticeable amounts of sulfur, but the amount varied appreciably around the pore edge. A high sulfur content was always associated with a higher Fe and/or Cr content, but higher magnification examination around the pores (Fig. 2b) did not reveal any precipitates. Hence, the Fe and Cr may be co-adsorbed with the S on these pore surfaces. Since S and Cr are abundantly found at Al_2O_3/FeCrAl interfaces due to co-segregation effects [12], these internal voids most likely nucleated at the interface in order to have incorporated these elements onto their surfaces. Similar intragranular voids have also been observed in Al_2O_3 grown on NiCrAl [24]. There the void size was found to increase with distance from the scale/alloy interface. This size distribution throughout the scale suggests that the pores formed at the scale/alloy interface and coalesced to larger sizes further away from the interface in an inwardly growing scale.

A possible mechanism for pore formation at the interface in the grain faces is illustrated in Fig. 3. The growth of the Al_2O_3 layer is dominated by the transport of O down oxide grain boundaries, with a minor contribution of Al outward diffusion [1,2]. In order to maintain compatible growth of all the grains at the scale/alloy interface, diffusion of O and counter diffusion of metal along the interface are necessary. In the case where the interface diffusivity of O is less than the rate at which O is transported down the grain boundary to the interface, a driving force for pore nucleation at the interior of the grain exists. It might be expected that the newly formed oxide would simply form a projection into the metal, analogous to the ridges that form on the free surface, Fig. 3. However, misfit stresses arise owing to the volume change. Gradients in these stresses as well as the interface curvature can drive diffusion along the interface and keep it flatter than occurs at the free surface. Although the normal stress acting across the oxide/metal interface must average zero, it can be compressive near the oxide grain boundary and tensile near the grain center and thereby drive the oxygen transport. When a pore is formed near the grain center, the diffusion distance along the slower path then decreases and the stresses are reduced. Once a small intragranular pore forms at the interface, its surface on the metal side and perhaps on the oxide side will be enriched with S that segregates from the alloy. The presence of this sulfur then stabilizes the void by reducing its surface energy [25]. As growth of the oxide scale continues inward, the void would be entrapped into the grain, leaving small amounts of S on the void surface. That is why within the scale S is only detected on the void surface but not anywhere else.

4. Conclusions

Iron and chromium are the major impurities present in Al_2O_3 scales formed on FeCrAl. Primarily their oxides formed during the transient stage and were incorporated into the α-Al_2O_3 scale. Fe segregated to some α-Al_2O_3 grain boundaries, but not Cr. The Al_2O_3 scale became progressively purer with oxidation time. It is possible that the Fe in the Al_2O_3 scale increases the scaling rate and, in particular, enhances lateral growth that causes scale convolution.

Sulfur was found at the scale/alloy interface, around internal voids within the oxide and on an occasional oxide grain boundary. At the latter two locations, it was present with the co-adsorption of Fe and/or Cr. This S distribution suggests that sulfur, which segregates to the scale/alloy interface, does not diffuse into the scale. Intragranular voids within the Al_2O_3 scale probably nucleated at the scale/alloy interface prior to being entrapped in the oxide grain. One driving force for their nucleation derives from stresses needed to enforce uniform scale growth when diffusivities at the oxide grain boundary are greater than along the interface.

Acknowledgement

This work was supported by the US Department of Energy, Office of Basic Energy Sciences under contract DE-AC03-76SF00098.

References

[1] Mennicke C, Schumann E, Ruhle M, Hussey RJ, Sproule GI, Graham MJ. Oxid. Metals 1998;49:455.

[2] Quaddakkers WJ, Elschner A, Speier W, Nickel H. Appl Surf. Sci 1991;52:271.

[3] Golightly FA, Stott FH, Wood GC. J Electrochem Soc 1979;126:1035.

[4] Przybylski K. Garrett-Reed AJ, Pint BA, Katz EP, Yurek GJ. J Electrochem Soc 1987;134:3207.

[5] Tolpygo, VK, Clarke, RD. High Temperature Corrosion and Materials Chemistry III, ECS, 2001. p.15.

[6] Cho J, Harmer MP, Chan HM, Richman JM, Thompson AM. J Am Ceram Soc 1997;80:1013.

[7] Wang CM, Cho J, Chan HM, Harmer P, Richman JM. J Am Cerem Soc 2001;84:1010.

[8] Lessing PA, Gordon RS. J Mater Sci 1977;12:2291.

[9] Hollenberg GW, Gordon RS. J Am Ceram Soc 1973;56:140.

[10] Gordon, RS. Adv. in Ceram 1984;10: 418.

[11] Cannon RM, Hou PY. High Temperature Corrosion and Materials Chemistry, The Electrochem. Soc., 1998. p.594.

[12] Hou PY. Mater and Corr 2000;51:329.

[13] Fox P, Lees DG, Lorimer GW. Oxid Metals 1991;36:491.

[14] Ben Abderrazik G, Moulin G, Huntz AM, Berneron R. J Mater Sci 1984;19:3173.

[15] Cliff G, Lorimer GW. J. Microsc. 1975;103:203.

[16] Andoh A, Taniguchi S, Shibata T. Materials Science Forum 2001;369-372:303.

[17] Ikeda JAS, Chiang YM, Garratt-Reed AJ, Vander Sande JB. J. Am. Ceram. Soc. 1993;76:2447.

[18] Levin EM, Robbins CR, McMurdie HF. Phase Diagram for Ceramists, The Am. Ceramic Soc Inc; 1964. Fig. 309.

[19] Muan A. Am J Sci 1958;256:413.

[20] Novokhatskii IA, Velov BF, Gorokh AV, Savinskaya AA. Russ J Phys Chem 1965;39:1498.

[21] Van Lienden C, Hou PY. unpublished results.

[22] Tolpygo VK, Clarke DR. Acta mater 1998;46:5153.

[23] See for example, Pint BA. Oxid Metals 1997;48:303.

[24] Smialek JL, Gibala R. High Temperature Corrosion, NACE, 1981. p.274.

[25] Halden FA, Kingery WD. J Phys Chem 1955;59:557.

Table 1: Fe and Cr concentrations in α-Al_2O_3 scales and effect on lattice parameters

Oxidation condition	Scale thickness[+] (μm)	Oxide grain size (nm)	Average [Cr] (at%)	Average [Fe] (at%)	Lattice parameter[*]
1000°C, 0.5h	0.39	107±36	4.12±0.95	4.49±1.67	a= 4.95±0.04 Å c=13.53±0.08 Å
1000°C, 1h	0.9	191±44	0.34±0.85	1.91±0.49	
1000°C, 26h	1.77	186±53	0.24±0.28	0.60±0.32	a= 4.75±0.04 Å c=13.47±0.08 Å
1200°C, 2h	2.94	**291±46**	**0.3±0.64**	0.70±0.57	
1200°C, 120h	4 – 5.5	1546±423	0.27±0.20	0.06±0.06	a= 4.71 ± 0.04Å c=13.23±0.08 Å

[+]Calculated from weight gain except the last sample where thickness was determined from SEM micrographs of scale cross sections.

[*]Standard parameters for α-Al_2O_3 are: a= 4.758 Å, c=12.991 Å.

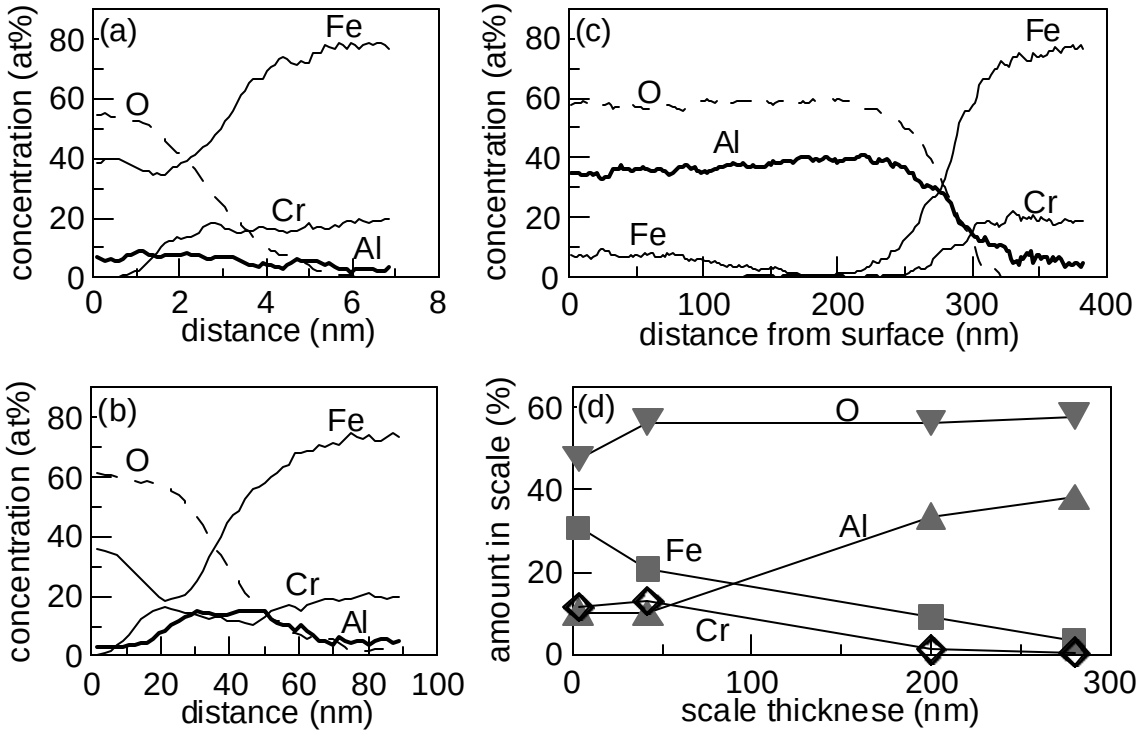

Figure 1: AES depth profiles of surface oxides on the FeCrAl after oxidation for: (a) starting surface, (b) 1 min, sample surface at T=670°C and (c) 11 min, T=1000°C. (d) Relative concentration of elements in the scale from integrating the curves in the oxide portion of depth profiles. The oxide/metal interface is located nominally (albeit imprecisely owing to oxide scale roughness) at the inflection points for O and Fe signals.

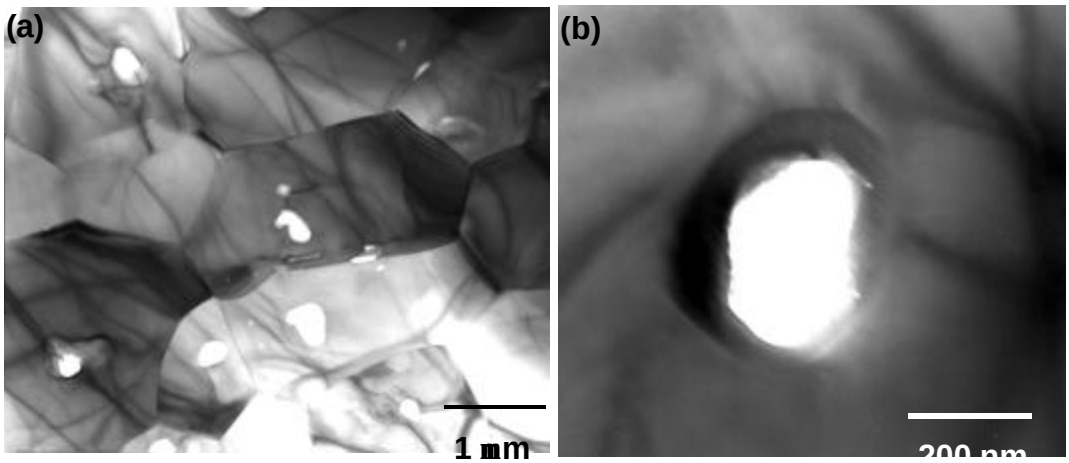

Figure 2: (a) TEM micrograph of the Al_2O_3 scale formed at 1200°C/120h after ion-mill thinning from both sides showing the presence of sub-micron sized intragranular voids. (b) Magnified view of a typical void.

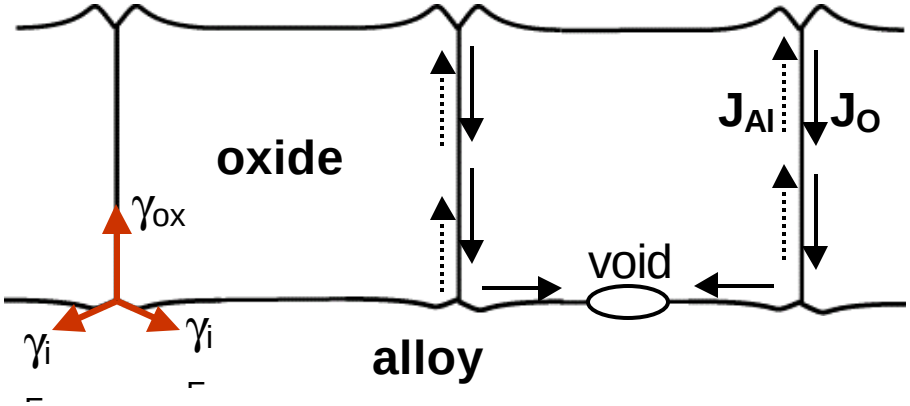

Figure 3: Schematic illustration of a mechanism of pore formation at the scale/alloy interface away from oxide grain boundaries. Pores that form when diffusion along the interface is slower

than that on the oxide grain boundaries will shorten diffusion distances and reduce the stresses acting across the oxide/metal interface.